A droplet manipulation on a liquid crystal and polymer composite film as a concentrator and a sun tracker for a concentrating photovoltaic system

Yu-Shih Tsou, Kai-Han Chang, and Yi-Hsin Lin

Citation: Journal of Applied Physics **113**, 244504 (2013); doi: 10.1063/1.4812391
View online: http://dx.doi.org/10.1063/1.4812391
View Table of Contents: http://scitation.aip.org/content/aip/journal/jap/113/24?ver=pdfcov
Published by the AIP Publishing

A droplet manipulation on a liquid crystal and polymer composite film as a concentrator and a sun tracker for a concentrating photovoltaic system

Yu-Shih Tsou, Kai-Han Chang, and Yi-Hsin Lin[a)]
Department of Photonics, National Chiao Tung University, 1001 Ta Hsueh Rd., Hsinchu 30010, Taiwan

(Received 9 May 2013; accepted 11 June 2013; published online 28 June 2013)

We demonstrate a droplet manipulation on a liquid crystal and polymer composite film (LCPCF) as a concentrator and a sun tracker for a concentrating photovoltaic (CPV) system with a steady output electric power. The CPV system adopts a liquid lens on LCPCF whose curvature is not only tunable but position is also bistably switchable based on liquid crystal orientations on LCPCF. The change of curvature of the liquid lens results in a tunable concentration ratio which helps to increase photocurrent at a low illumination and prevent the effect of the series resistance at a high illumination. Moreover, the change of the position of the liquid lens helps to track sun owing to sun movement. Therefore, the output power of such a system is steady no matter the sunlight condition and the angle of incident light. The operating principles and experiments are investigated. The concept in this paper can be extended to design optical components for obtaining steady output power of the solar cell at indoor or outdoor use and also tracking sunlight. © *2013 AIP Publishing LLC*. [http://dx.doi.org/10.1063/1.4812391]

I. INTRODUCTION

Solar cells convert the energy of sunlight directly into electricity.[1] The output power generated by conventional solar cells is low, especially at a cloudy day or at an indoor condition. To increase the irradiance of incident light, a concentrating photovoltaic (CPV) system, a solar cell combined with a concentrating device, is adopted.[2] A CPV system can focus light over a large area into a small area of a solar cell; nevertheless, the CPV system needs an extra sun tracker in order to guide the sunlight to the solar cells due to the movement of sun. Two kinds of solar trackers are developed, such as a Fresnel lens combined with a mechanically tilting plate and microlens arrays combined with a mechanically positional shifter.[3–5] However, both of sun trackers are bulky and need mechanical moving part. Moreover, the output electricity changes under different sunlight condition and the different incident angles of sun[6,7] owing to three main reasons: (1) insufficient photocurrents at a low illumination, (2) an effect of the series resistance induced by over saturation of incident photon flux, and (3) an obliquely incident light under sun movement. Therefore, it is important to develop a sun-tracking CPV system with a high and stable output electric power under both of changes of sunlight conditions and changes of sunlight movements. Recently, we demonstrated a concept of a CPV system with a liquid crystal (LC) lens whose concentration ratio is adjustable in order to overcome the effect of insufficient photocurrents and the effect of the series resistance under different sunlight conditions.[8–19] As a result, the output electric power of such a CPV system is maximal and static under different sunlight conditions. Although the CPV system generates high electric power indoors as well as outdoors, it still requires an extra sun tracker for the sun movement, such as a positional shifter for the LC lens. Hence, the CPV system needs an optical device with both of a tunable concentration ratio and a lateral positional shifter. In these years, we developed a liquid crystal and polymer composite film (LCPCF) whose surface free energy is switchable owing to LC orientations and several applications based on droplet manipulation on LCPCF were developed as well, such as electro-optical switches, sperm testing devices, and liquid lenses.[16,20–24] In this paper, we demonstrate a CPV system with a steady output electric power. The curvature of the liquid lens can be adjusted to affect the concentration ratio and the position of the liquid lens can also be bistably controlled to track the sunlight. As a result, the output power of the CPV system remains maximally by controlling the orientations of LCs on LCPCF under various conditions of sunlight and under the sunlight movement. The operating principles are investigated and the concept is demonstrated experimentally. The concept in this paper can provide a guideline to design optical components for obtaining steady output power of the solar cell under variety of sunlight.

II. OPERATING PRINCIPLES

The operating principles of the proposed CPV system are illustrated in Figs. 1(a)–1(d). In Fig. 1(a), we illustrate the mechanism of the liquid lens based on the droplet manipulation on LCPCF. A fluidic drop is placed on the LCPCF and a patterned indium tin oxide (ITO) glass substrate with three electrode regions is set underneath, as shown in Fig. 1(a). The patterned ITO glass substrate provides fringe electric fields at the surface of LCPCF. The ITO electrodes on the glass substrate were etched with interdigitated chevron patterns, shown as the zigzag electrodes in the Fig. 1(a). The zigzag ITO strips have corner angles of 150°. The width and gap of the electrode strips are 4 μm and 14 μm, respectively. In order to manipulate a fluidic drop on LCPCF, the three regions of the interdigitated chevron electrodes were patterned identically, as shown in Fig. 1(a). The main

[a)]Electronic mail: yilin@mail.nctu.edu.tw

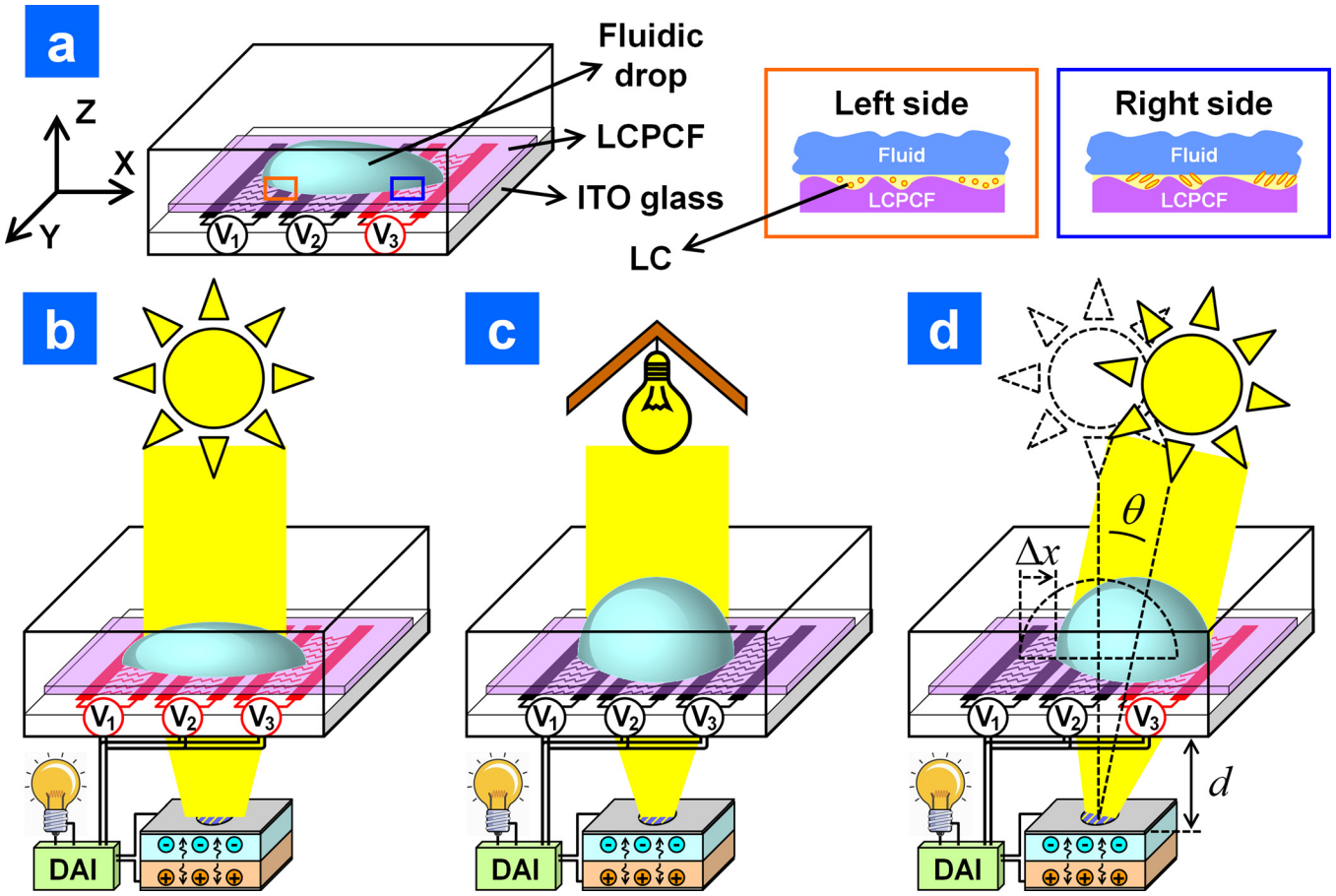

FIG. 1. Operating principles of the droplet manipulation on LCPCF for CPV system. (a) The fluidic drop on LCPCF can be manipulated by applied pulsed voltages because of the orientations of LC molecules. The left square inlet indicates the orientations of LC molecules are parallel to y-axis at voltage-off state. The right inlet indicates the tilt of LC molecules at voltage-off state. The droplet manipulation on LCPCF or the liquid lens in (a) is operated (b) with a low concentration ratio under strong illumination, and (c) with a high concentration ratio under weak illumination. (d) The liquid lens shifts the location at the oblique incidence of sunlight.

concept of the electrode design is to provide electric fields to change the orientations of LC molecules on LCPCF. The width, distance, and corner angles of the electrodes affect the translational distance and the velocity of the fluidic drop. The fluidic drop is originally located in the middle of the three electrode regions. When we apply a pulsed voltage to the right side of the LCPCF (i.e., V_3) in Fig. 1(a) for example, the fluidic drop moves to the right because the right region is more hydrophilic or surface free energy of the right region is higher resulting from the tilts of the LC orientations as shown in the two square inlets of Fig. 1(a). The relation between electrically tunable surface free energy of LCPCF and the LC orientations is discussed previously.[25] When we apply the identical pulsed voltages to V_1, V_2, and V_3, the fluidic drop changes its curvature only without moving. When the fluidic drop is applied pulsed voltages to V_3 and V_1 by turns, the fluidic drop moves to the right region and the left region accordingly. As a result, the functions of the fluidic drop on LCPCF cannot only be an electrically tunable focusing liquid lens due to the change of the curvature, but also control the shift of focusing spot along the focusing plane which usually is the plane of the solar cell located due to the change of the position of the fluidic drop. This also means the liquid lens on LCPCF can not only be a concentrator but also a sun tracker. Then the liquid lens in Fig. 1(a) is placed on the top of a multi-junction solar cell as shown in Figs. 1(b)–1(d). In Figs. 1(b) and 1(c), when the sunlight passes through the liquid lens, the liquid lens changes the curvature by applying different homogeneous voltages (i.e., $V_1 = V_2 = V_3 \equiv V_{total}$) to modulate the number of photons over an area and over a period of time (i.e., photon-flux density) to the solar cell. The absorbed photons in the depletion region of the solar cell generate the free electrons and holes to form a photocurrent which can be further converted into an alternating current (AC) by a DC-AC inverter (DAI). Such an alternating current provides electricity to LCPCF and a bulb (or other devices). The radius of curvature of the liquid lens is large, which corresponds to a lower concentration ratio as a concentrator. We use the lower concentration ratio of the liquid lens under strong sunlight to prevent the effect of the series resistance at a high illumination. Under weak illumination, such as indoor environment as depicted in Fig. 1(c), the concentration ratio of the liquid lens is increased by decreasing V_{total} in order to increase photocurrent at a low illumination. In this way, the conditions in Figs. 1(b) and 1(c) are able to have the same electric output power. However, sun moves. Under the movement of sun, the oblique sunlight results in a decrease of the output power of

the solar cell. In order to compensate the oblique effect of the sunlight, we shift the position of the liquid lens in order to shift the oblique sunlight back to the solar cell according to the droplet manipulation on LCPCF as shown in Fig. 1(d). Even though oblique sunlight changes the irradiance due to the change of the ambient conditions (i.e., indoor or outdoor), we can shift the position of liquid lens and change the radius of curvature simultaneously to maintain the generated output power.

To prove the operating principles, we assume the oblique angle of the sun is θ with respect to the normal direction of the solar cell, and is θ' with respect to the normal direction of the liquid lens, as shown in Figs. 2(a) and 2(b). The distance between the liquid lens and the solar cell is d. As a result, the focused sunlight shifts a distance of $d \times \tan\theta'$, as shown in Fig. 2(a). In order to compensate the oblique effect of sunlight, the liquid lens moves a distance of $\Delta x(V_3)$ by applying a pulsed voltage of V_3, as depicted in Fig. 2(b). From Fig. 2(b), $\Delta x(V_3)$ equals to $d \times \tan\theta$. Assume the mean photon-flux density (φ_{onesun}) is ~1 mW/mm^2 as the sun is on the top of the liquid lens and the solar cell, and S is a sunlight factor which indicates the variation of sunlight depending on weather conditions. The photon-flux density (φ_{input}) accepted by the solar cell at the oblique incidence is expressed as,

$$\varphi_{input} = \varphi_{onesun} \times S \times \cos\theta \times C(V_{total}), \quad (1)$$

where C is a voltage-dependent concentration ratio of the liquid lens, defined as the area ratio of the liquid lens to the solar cell at the normal incidence. The oblique effect of sunlight is considered by multiplying $\cos\theta$ in Eq. (1). In our previous study, to achieve the maximum of the output electrical power density, φ_{input} should be satisfied,[8]

$$k_B \times T/q \times FF \times \left\{ \ln\left[\frac{\varphi_{input}}{\varphi_{onesun}}\right] + 1 \right\} - 2 \times \frac{\varphi_{input}}{\varphi_{onesun}} \times J_{SC,1} \times R_S + FF \times V_{OC,1} = 0, \quad (2)$$

where k_B is Boltzmann's constant (1.38×10^{-23} J K^{-1}), T is temperature in Kelvin, q is the electron charge, *FF* is the fill factor, R_S is the series resistance, $J_{SC,1}$ and $V_{OC,1}$ denote the short circuit current and open circuit voltage at $\varphi_{input} = \varphi_{onesun}$, respectively. The solution of φ_{input} in Eq. (2) is a constant, defined as φ_S, because the other parameters in Eq. (2) are fixed. From Eq. (1), φ_S equals to $\varphi_{onesun} \times S \times \cos\theta \times C(V_{total})$. Under a normal incidence (i.e., $\theta = 0$), we adjust concentration ratio $C(V_{total})$ satisfying: $C(V_{total}) = \varphi_S/(\varphi_{onesun} \times S)$ in order to maintain the maximum of P_{out} no matter the sunlight condition S. Under an oblique incidence (i.e., $\theta \neq 0$), we move the liquid lens in a distance of $\Delta x(V_3) (= d \times \tan\theta)$ by applying voltage V_3 and then re-adjust the concentration ratio $C(V_{total})$ satisfying $C(V_{total}) = \varphi_S/(\varphi_{onesun} \times S \times \cos\theta)$. In this way, P_{out} is still a maximum. Therefore, manipulating the concentration ratio and the location of a droplet on LCPCF can be used as a concentrator and a sun tracker for CPV system at the same time for obtaining a steady and maximum output electric power.

III. EXPERIMENTAL RESULTS AND DISCUSSION

To demonstrate the concept of the proposed CPV system, we prepared the LCPCF with the liquid lens. To fabricate LCPCF, we prepared an empty cell consists of a patterned ITO glass substrate and a glass substrate coated with a mechanically buffered polyimide layer. Then we filled the cell with a mixture containing of a nematic LC mixture E7 (Merck) and a liquid crystalline monomer (4-(3-Acryloyloxypropyloxy)-benzoic acid 2- methyl-1, 4-phenylene ester) at 70:30 wt. % ratios, and the cell is exposed to a UV light. After phase separation and photo-polymerization, the top glass substrate was peeled off by a thermal-releasing process. A drop of DI water of 6 μl was dropped on the solidified LCPCF to form a liquid lens. The device was assembled using another glass substrate to avoid the evaporation of the liquid lens.

To measure the moving distance (Δx) of the liquid lens induced by the inhomogeneous surface free energy of LCPCF, we applied a pulsed voltage to LCPCF and recorded the dynamics of the droplet by a CCD camera (JAI CV-M30) with a frame rate of 120 frames/s. In the beginning, the droplet is placed in the middle of the three electrode regions. We then applied a square pulsed voltage of 200 V_{rms} to V_3 and V_1 by turns with a time duration of 1 s and the frequency (f) of 1 kHz. The results are shown in Figs. 3(a) and 3(b). At t = 1 s, the droplet moved to a distance of 0.9 mm when we applied the pulsed voltage of $V_3 = 100$ V_{rms}. As we turned off the voltage (i.e., $V_3 = 0$) at t = 2 s, the liquid lens stayed at the distance of 0.9 mm. At t = 3 s, the

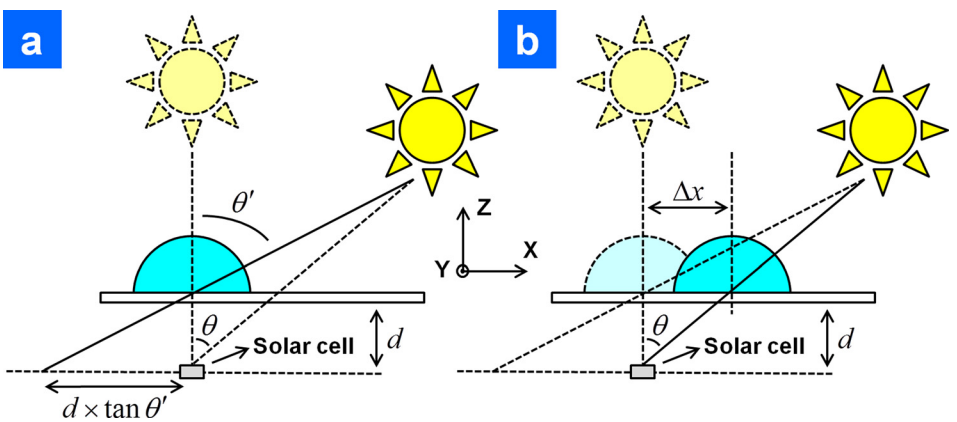

FIG. 2. The illustration of the sun-tracking mechanism by using the movement of liquid lens. (a) When the incident angle of sunlight change, the focusing spot shift a distance of $d \times \tan\theta'$. (b) To shift the focusing spot back to the solar cell, the liquid lens shifts a distance of Δx.

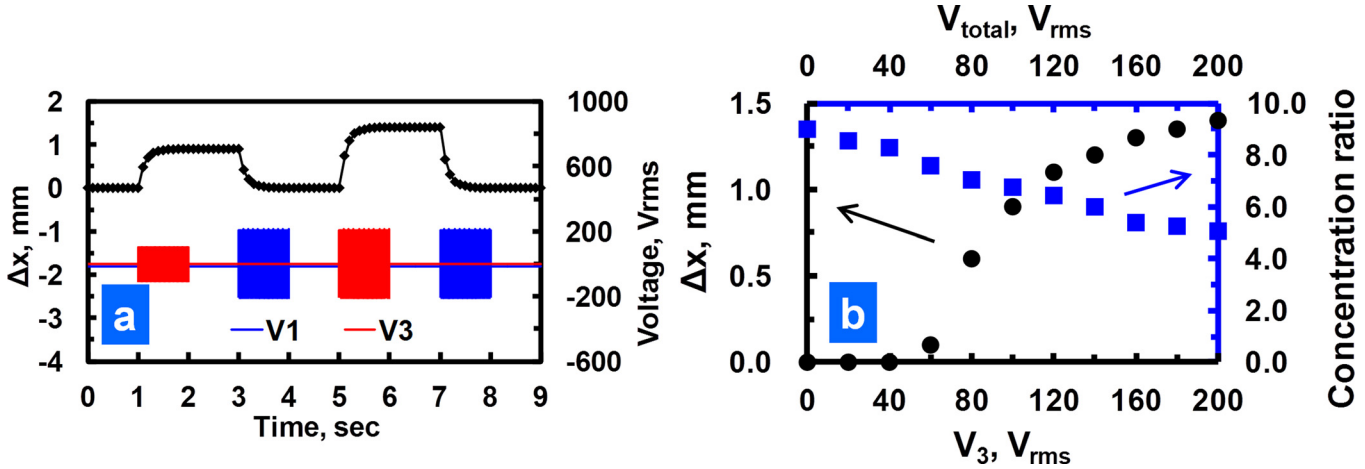

FIG. 3. (a) The moving distance (Δx) of the liquid lens as a function of an applied pulsed voltage of (V_1, V_3) of LCPCF. (b) The moving distance of the liquid lens as a function of the amplitude of V_3 (black dots) and the concentration ratio of the liquid lens as a function of V_{total} (blue squares).

droplet moved back to the initial location (i.e., $\Delta x = 0$) when the applied voltages of $V_1 = 200$ V_{rms} and $V_3 = 0$ V_{rms}. At $t = 4$ s, the droplet stayed at the initial location even though we turned off the voltages. The position of the droplet can be manipulated bistably by controlling the applied voltages. We also measured the moving distance of Δx as a function of the amplitude of V_3, as shown in black dots in Fig. 3(b). When the applied voltage exceeds the threshold voltage ($V_{th} \sim 50$ V_{rms}), the moving distance Δx of the droplet increases with the amplitude of V_3. The maximum moving distance is around 1.4 mm, which is limited by the distance between the left and the right electrodes (i.e., electrode regions of applied V_1 and V_3). The moving distance can be improved by the electrode design.

To measure the concentration ratio of the liquid lens, we applied a homogeneous electric field ($V_{total} = V_1 = V_2 = V_3$) and recorded the dynamics of the droplet by the same CCD camera. When we applied voltages to the LCPCF, we measured the radius of curvature of the droplet of the liquid lens. According to the radius of curvature, we calculated the focal length of the liquid lens and then calculated the concentration ratio by geometrical optics. The results are shown in blue squares in Fig. 3(b). In Fig. 3(b), the concentration ratio of the liquid lens is modulated from ~5 to ~9 by controlling V_{total} from 200 V_{rms} to 0 V_{rms}. The concentration ratio can be improved by increasing the volume of the liquid lens or refractive index of the liquid

To measure the output power density of the CPV system, a white light source (Taiwan Fiber Optics, LSH-150F, irradiance ~1 mW/mm^2) was used to mimic the sunlight and to illuminate the liquid lens. The structure of the solar cell was GaInP/GaInAs/Ge triple junction (Arima, Model T3JG6F055011) with a wavelength range: 350–1800 nm and the diameter of 1 mm. The solar cell was placed at d = 3.2 mm behind the liquid lens and connected to a power supply (Agilent, E3631A) and a multi-meter (Agilent, 34401 A), as depicted in Fig. 1(b). We first measured the current-voltage (I-V) curve of the solar cell and then calculated the output power density as a function of the voltage. From the relation between the output power density and the voltage, we chose the maximum output power density defined as P_{out}.[8] We measured P_{out} as a function of the concentration ratio of the liquid lens by applying voltage under different sunlight condition (S), as shown in Fig. 4(a). S is defined as the ratio of the irradiance of the light source to the irradiance of 1 sun (~1 mW/mm^2). From Fig. 4(a), the P_{out} increases with the concentration ratio first due to photovoltaic effect and then decreases after reaching a maximum due to series resistance effect.[8] The concentration ratio to achieve maximum P_{out} (~325 μW/mm^2) for S = 1, 0.85, and 0.7 are 6.4, 7.6, and 9.0, respectively. This means the solar cell generates the highest output power density (i.e., 325 μW/mm^2 in Fig. 4(a)) under different sunlight condition as long as we adjust the concentration ratio of the liquid lens without moving the location of the liquid lens (i.e., $\Delta x = 0$ in Figs. 1(d) and 2(b)).

Next, we moved the location of the liquid lens in order to see the change of P_{out} under different angle of sunlight (i.e., θ in Figs. 1(d) and 2(b)). The P_{out} as a function of moving distance is shown in Fig. 4(b). At the normal incidence (i.e., $\theta = 0°$), the output power density decreases with the moving distance Δx because the focusing spot of sunlight after passing through the liquid lens shifts away from the solar cell. At $\theta = 10°$, P_{out} has a maximum of 322 μW/mm^2 when $\Delta x = 0.6$ mm. At $\theta = 20°$, P_{out} has a maximum of 310 μW/mm^2 when $\Delta x = 1.2$ mm. At $\theta = 25°$, P_{out} has a maximum of 302 μW/mm^2 when $\Delta x = 1.4$ mm. As a result, we can change the position of the liquid lens to trace the sun in order to obtain the maximum output power density. From Fig. 4(b), we plotted the moving distance Δx when P_{out} is maximal as a function of incident angle θ, as shown in black dots in Fig. 5. We also plotted theoretical Δx as a function of $d \times \tan\theta$ (d is 3.2 mm in our experiments) in black dotted line in Fig. 5. The experimental results and theoretical results are similar. Therefore, no matter where the sun is, we can obtain local maximum P_{out} in Fig. 4(b) by moving the liquid lens. We also plotted the local maximum P_{out} in Fig. 4(b) as a function of incident angle, as shown in the green dotted line with squares in Fig. 5. Actually, the local maximum P_{out} decreases ~93% when the incident angle changes from 0° to 25°. This is because the oblique light results in the decrease of the photon flux density (i.e., photon numbers per unit area per unit time). For comparison, we also measured P_{out} as a function of the incident angle without the location change of

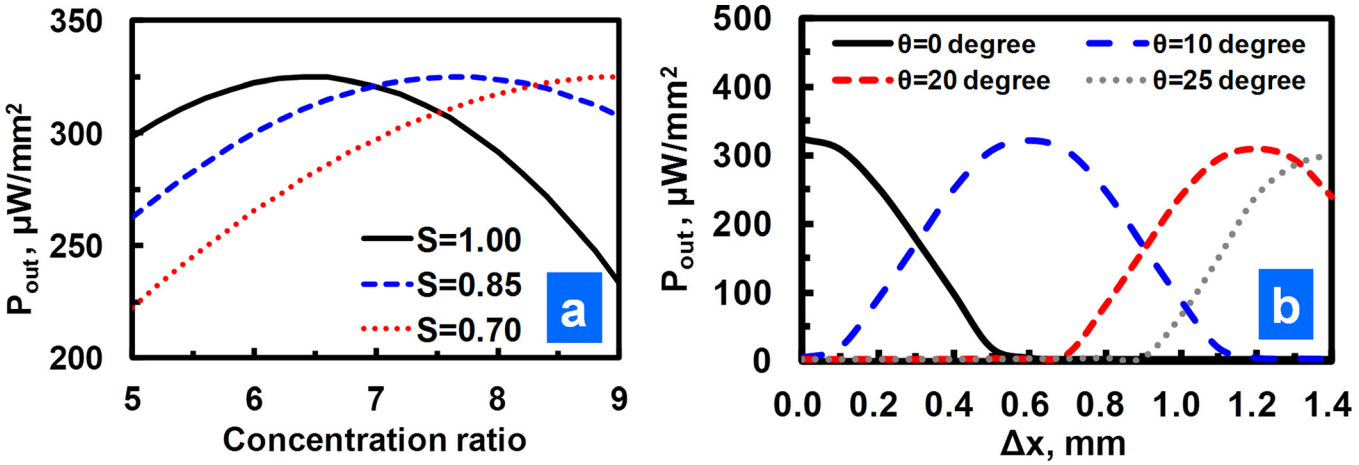

FIG. 4. (a) Output power density as a function of the concentration ratio under different sunlight conditions. (b) Output power density as a function of the moving distance at different incident angles when S = 1 and C = 6.4.

liquid lens (the red dotted line with triangles). As we can see, the output power density drops dramatically at $\theta > 5°$ at $\Delta x = 0$. However, the output power density drops slowly when we adjust the location of the liquid lens. As a result, the output power density drops only 93% even the incident angle is 25°.

In order to obtain the steady output power density without decrease of 93% as the incident angle changes, we can move the liquid lens to trace the sun first and then adjust the concentration ratio of the liquid lens to improve the output power density. In the experiments, we controlled the angle of the incident light (i.e., θ) and then moved the liquid lens Δx according to the black dotted line in Fig. 5. After that, we measured the output power density when changing the concentration ratio of the liquid lens. The output power density as a function of the concentration ratio of the liquid lens is depicted in Fig. 6. Fig. 6 indicates that the output power density can have local maximum by adjusting the concentration ratio of the liquid lens at the different incident angle which requires the different location of the liquid lens. Moreover, the local maximums of four curves are identical $\sim 325\ \mu W/mm^2$. We also plotted P_{out} as a function of incident angle after manipulating both of the position and the concentration ratio of the liquid lens, as shown in blue dotted line with diamonds in Fig. 5. Therefore, we can manipulate the position of the liquid lens to trace sun and then change the concentration ratio of the liquid lens to obtain the steady output power density. In other words, we can have a steady output power of the solar cell in spite of sun movement by manipulating the motion and the curvature of the liquid lens.

According to the experimental results in Fig. 6, the maximum φ_{input} in the system is around 6.4 mW/mm^2, which is calculated by putting the experimental parameters back to Eq. (1): S = 1, $\theta = 0°$, and C = 6.4. We can also estimate the theoretical value of the maximum φ_{input} by means of putting related parameters into Eq. (2): T = 300 K, $q = 1.6 \times 10^{-19}$ C, FF = 0.85, $J_{SC,1} = 4$ mA, $V_{OC,1} = 2.37$ V, and $R_S = 40\ k\Omega$. The theoretical φ_{input} (i.e., φ_S) is around 6.5 mW/mm^2 which is similar to the experimental result (6.4 mW/mm^2). This also means the liquid lens using droplet manipulation on LCPCF is not only a concentrator but also sun tracker to make the output power density in the CPV system steady and maximal. In order to operate the liquid lens on LCPCF, we have to apply voltage which consumes the energy as well. As to the power consumption of the liquid lens on LCPCF, the measured power consumption of LCPCF was less than $1\ \mu W/mm^2$ at any applied voltage of LCPCF.

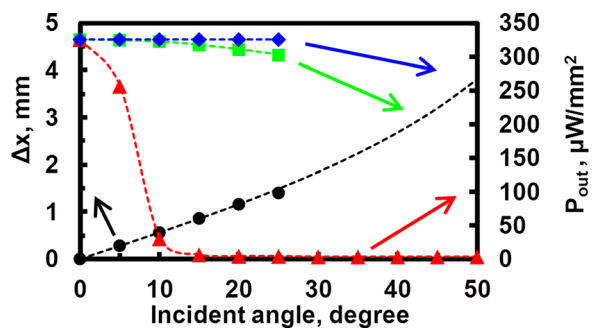

FIG. 5. The moving distance as a function of incident angle (black dots). The output power density as a function of incident angle when $\Delta x = 0$ mm (red triangles). Output power density as a function of incident angle with the manipulation of the moving distance Δx of the liquid lens (green squares). The output power density as a function of incident angle with the manipulation of both of moving distance Δx and the concentration ratio C (blue diamonds).

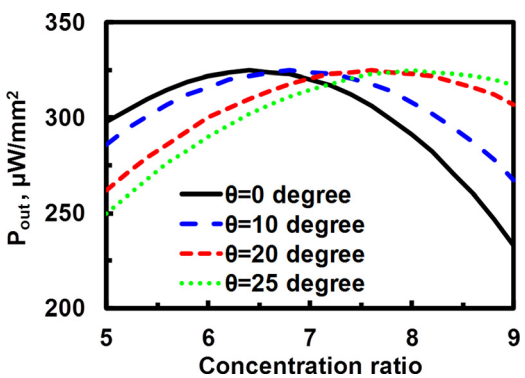

FIG. 6. The output power density as a function of concentration ratio at different incident angles and at related moving distance Δx. The relation between incident angles and the moving distance is plotted in the black dots in Fig. 5.

Compared to the output power density $\sim 325\,\mu W/mm^2$, the energy gain is larger than $\sim 300\,\mu W/mm^2$ and the power consumption of the liquid lens on LCPCF can be neglected.

IV. CONCLUSION

A CPV system with a steady electrical output adopting a droplet manipulation on a LCPCF, a liquid lens, as a concentrator and a sun tracker was demonstrated. On the basis of changing the concentration ratio and location of the liquid lens on LCPCF, the CPV system can be operated in the fixed and maximum output power density under different irradiance and incident angles of sunlight. To further improve output power density, both the areas of the solar cell and the aperture size of the liquid lens should be increased in order to increase the concentration ratio. Improving the materials of solar cells with better performance is also a way to go. To improve the sun-tracking angle ($\pm 25^\circ$ in our experiments), we can increase the moving distance of the liquid lens (i.e., Δx) by means of better electrode design, arrays designs of the CPV system or increase the concentration ratio of the liquid lens.[26] For the practical application of large sized solar cell modules, we can use arrays of liquid lens on LCPCF combined with solar cell arrays. Each individual liquid lens on LCPCF is in charge of individual solar cell of the solar cell arrays. In this way, the output power can be further enlarged. The concept we proposed can not only provide a guideline to design other optical components for obtaining steady output power of the solar cell under variety of sunlight, but also be applied to design image stabilization system for the cameras and cell phones.

ACKNOWLEDGMENTS

The authors are indebted to Dr. An-Chi Wei (National Central University) for the discussions. This research was supported by the National Science Council (NSC) in Taiwan under Contract No. 101-2112-M-009-011-MY3.

[1]L. El Chaar, L. A. lamont, and N. El Zein, "Review of photovoltaic technologies," Renewable Sustainable Energy Rev. **15**, 2165 (2011).
[2]W. T. Xie, Y. J. Dai, R. Z. Wang, and K. Sumathy, "Concentrated solar energy applications using Fresnel lenses: A review," Renewable Sustainable Energy Rev. **15**, 2588 (2011).
[3]C. Y. Lee, P. C. Chou, C. M. Chiang, and C. F. Lin, "Sun tracking systems: a review," Sensors **9**, 3875 (2009).
[4]F. Duerr, Y. Meuret, and H. Thienpont, "Tracking integration in concentrating photovoltaics using laterally moving optics," Opt. Express **19**, A207 (2011).
[5]Y. H. Lin and Y. S. Tsou, "A polarization independent liquid crystal phase modulation adopting surface pinning effect of polymer dispersed liquid crystals," J. Appl. Phys. **110**, 114516 (2011).
[6]A. Cheknane, H. S. Hilal, J. P. Charles, B. Benyoucef, and G. Campet, "Modelling and simulation of InGaP solar cells under solar concentration: Series resistance measurement and prediction," Solid State Sci. **8**, 556 (2006).
[7]P. Peumans and S. R. Forrest, "Very-high-efficiency double-heterostructure copper phthalocyanine/C60 photovoltaic cells," Appl. Phys. Lett. **79**, 126 (2001).
[8]Y. S. Tsou, Y. H. Lin, and A. C. Wei, "Concentrating photovoltaic system using a liquid crystal lens," IEEE Photon. Technol. Lett. **24**, 2239 (2012).
[9]Y. H. Lin and H. S. Chen, "Electrically tunable-focusing and polarizer-free liquid crystal lenses for ophthalmic applications," Opt. Express **21**, 9428 (2013).
[10]H. C. Lin, N. Collings, M. S. Chen, and Y. H. Lin, "A holographic projection system with an electrically tuning and continuously adjustable optical zoom," Opt. Express **20**, 27222 (2012).
[11]Y. H. Lin and M. S. Chen, "A pico projection system with electrically tunable optical zoom ratio adopting two liquid crystal lenses," J. Display Technol. **8**, 401 (2012).
[12]H. C. Lin and Y. H. Lin, "An electrically tunable-focusing liquid crystal lens with a low voltage and simple electrodes," Opt. Express **20**, 2045 (2012).
[13]H. C. Lin, M. S. Chen, and Y. H. Lin, "An electrically tunable focusing pico projection system based on a liquid crystal lens adopting a liquid crystal and polymer composite film," J. Nonlinear Opt. Phys. Mater. **20**, 477 (2011).
[14]H. C. Lin, M. S. Chen, and Y. H. Lin, "A review of electrically tunable focusing liquid crystal lenses," Trans. Electr. Electron. Mater. **12**, 234 (2011).
[15]Y. H. Lin, M. S. Chen, and H. C. Lin, "An electrically tunable optical zoom system using two composite liquid crystal lenses with a large zoom ratio," Opt. Express **19**, 4714 (2011).
[16]H. C. Lin and Y. H. Lin, "An electrically tunable focusing liquid crystal lens with a built-in planar polymeric lens," Appl. Phys. Lett. **98**, 083503 (2011).
[17]H. C. Lin, M. S. Chen and Y. H. Lin, "An electrically tunable focusing pico projector using a liquid crystal lens as an active optical element," Mol. Cryst. Liq. Cryst. **544**, 150 (2011).
[18]H. C. Lin and Y. H. Lin, "A fast response and large electrically tunable-focusing imaging system based on switching of two modes of a liquid crystal lens," Appl. Phys. Lett. **97**, 063505 (2010).
[19]H. C. Lin and Y. H. Lin, "An electrically tunable focusing pico projector," J. Jpn. Appl. Phys. **49**, 102502 (2010).
[20]Y. H. Lin, H. Ren, Y. H. Wu, S. T. Wu, Y. Zhao, J. Fang, and H. C. Lin, "Electrically tunable wettability of liquid crystal/polymer composite films," Opt. Express **16**, 17591 (2008).
[21]Y. H. Lin, H. Ren, Y. H. Wu, Y. Zhao, J. Fang, Z. Ge, and S. T. Wu, "Polarization-independent phase modulator using a thin polymer-separated double-layered structure," Opt. Express **13**, 8746 (2005).
[22]Y. H. Lin, H. Ren, S. Gauza, Y. H. Wu, Y. Zhao, J. Fang, and S. T. Wu, "IPS-LCD using a glass substrate and an anisotropic polymer film," J. Display Technol. **2**, 21 (2006).
[23]Y. H. Lin, J. K. Li, T. Y. Chu, and H. K. Hsu, "A bistable polarizer-free electro-optical switch using a droplet manipulation on a liquid crystal and polymer composite film," Opt. Express **18**, 10104 (2010).
[24]Y. H. Lin, T. Y. Chu, W. L. Chu, Y. S. Tsou, Y. P. Chiu, F. Lu, W. C. Tsai, and S. T. Wu, "A sperm testing device on a liquid crystal and polymer composite film," J. Nanomed. Nanotechnol. **S9**, 001 (2011).
[25]Y. H. Lin, T. Y. Chu, Y. S. Tsou, K. H. Chang, and Y. P. Chiu, "An electrically switchable surface free energy on a liquid crystal and polymer composite film," Appl. Phys. Lett. **101**, 233502 (2012).
[26]K. A. Baker, J. H. Karp, E. J. Tremblay, J. M. Hallas, and J. E. Ford, "Reactive self-tracking solar concentrators: concept, design, and initial materials characterization," Appl. Opt. **51**, 1086 (2012).